

Agro-meteorological risks to maize production in Tanzania: sensitivity of an adapted water requirements satisfaction index (WRSI) model to rainfall

Article

Accepted Version

Creative Commons: Attribution-Noncommercial-No Derivative Works 4.0

Tarnavsky, E. ORCID: <https://orcid.org/0000-0003-3403-0411>, Chavez, E. and Boogaard, H. (2018) Agro-meteorological risks to maize production in Tanzania: sensitivity of an adapted water requirements satisfaction index (WRSI) model to rainfall. International Journal of Applied Earth Observation and Geoinformation, 73. pp. 77-87. ISSN 0303-2434 doi: 10.1016/j.jag.2018.04.008 Available at <https://centaur.reading.ac.uk/77771/>

It is advisable to refer to the publisher's version if you intend to cite from the work. See [Guidance on citing](#).

Published version at: <https://www.sciencedirect.com/science/article/pii/S0303243417302829>

To link to this article DOI: <http://dx.doi.org/10.1016/j.jag.2018.04.008>

Publisher: Elsevier

All outputs in CentAUR are protected by Intellectual Property Rights law, including copyright law. Copyright and IPR is retained by the creators or other copyright holders. Terms and conditions for use of this material are defined in

the [End User Agreement](#).

www.reading.ac.uk/centaur

CentAUR

Central Archive at the University of Reading

Reading's research outputs online

Agro-meteorological Risks to Maize Production in Tanzania: sensitivity of an adapted water requirements satisfaction index (WRSI) model to rainfall

Abstract

The water requirements satisfaction index (WRSI) – a simplified crop water stress model – is widely used in drought and famine early warning systems, as well as in agro-meteorological risk management instruments such as crop insurance. We developed an adapted WRSI model, as introduced here, to characterise the impact of using different rainfall input datasets, ARC2, CHIRPS, and TAMSAT, on key WRSI model parameters and outputs. Results from our analyses indicate that CHIRPS best captures seasonal rainfall characteristics such as season onset and duration, which are critical for the WRSI model. Additionally, we consider planting scenarios for short-, medium-, and long-growing cycle maize and compare simulated WRSI and model outputs against reported yield at the national level for maize-growing areas in Tanzania. We find that over half of the variability in yield is explained by water stress when the CHIRPS dataset is used in the WRSI model ($R^2 = 0.52$ - 0.61 for maize varieties of 120-160 days growing length). Overall, CHIRPS and TAMSAT show highest skill ($R^2 = 0.46$ - 0.55 and 0.44 - 0.58 , respectively) in capturing country-level crop yield losses related to seasonal soil moisture

deficit, which is critical for drought early warning and agro-meteorological risk applications.

Keywords: WRSI, Rainfall, Remote sensing, Tanzania, Maize

1. Introduction

Inter-annual and seasonal rainfall and temperature variability affects crop-land and pasture productivity, particularly in regions of rainfed agriculture. Understanding the impacts of agro-meteorological risks such as drought on crop production requires detailed evaluation of the sensitivity of yield indicators and crop models to different datasets providing model inputs. For example, a rainfall dataset that erroneously detects a delayed season onset would reduce the length of the growing season, subsequently leading to simulations of yield reduction or failure in years of 'normal' rainfall.

The WRSI Model. The Water Requirements Satisfaction Index (WRSI) is perhaps the most widely used crop water balance technique in operational drought monitoring, in which rainfall variability is the main driver of changes in yield. WRSI was developed by the United Nations (UN) Food and Agricultural Organization (FAO) for use with synoptic station data to monitor rainfed croplands throughout the growing season (Doorenbos and Kassam 1979 in [Senay 2008](#); [Frere and Popov 1979](#)). Calibrated for a range of crops, WRSI, a.k.a. crop specific drought index (CSDI) ([Melesse et al., 2007](#)), provides an indication of crop performance on the basis of water availability during the growing season (Frere and Popov 1986 in [McNally et al. 2015](#)).

20 Through the relative relationship between water demand and supply, WRSI
21 indicates the extent to which crop water requirements are met during the
22 growing season ([Patel et al., 2011](#)).

23 *WRSI Applications.* WRSI forms the basis of the FAO AgroMet Shell tool
24 ([Patel et al., 2011](#)) and the FAOINDEX software (Gommes 1993 in [Rojas
25 et al. 2005](#)); a variation of WRSI is incorporated in the AquaCrop model
26 ([Steduto et al., 2012](#)) and the European Commission’s Joint Research Cen-
27 tre use WRSI for Africa and globally for in-house analyses. As part of an UN
28 World Food Programme effort to set up in-country food security monitoring
29 and early warning systems, WRSI is used in the Ethiopian Livelihood Early
30 Assessment and Protection (LEAP) system - a platform for early warning
31 owned by the Disaster Risk Management and Food Security Sector of the
32 Ministry of Agriculture in Ethiopia. Since the 2000s, WRSI has supported
33 the parametric agricultural insurance analysis of the Africa Risk Capacity,
34 a Specialised Agency of the African Union supporting weather risk man-
35 agement ([Bryla and Syroka, 2007](#); [Bastagli and Harman, 2015](#)). WRSI has
36 been used perhaps most extensively by the growing international user com-
37 munity of the US Agency for International Development (USAID) Famine
38 Early Warning System NETwork (FEWS NET), launched as FEWS in 1985
39 for five countries in the Sahel and Sudan ([Verdin and Klaver, 2002](#)) and
40 renamed to FEWS NET in 2000. The FEWS NET community employs a
41 ‘convergence of evidence’ approach where WRSI, alongside independent in-
42 formation from satellite-based records on rainfall and vegetation, provides

43 information on agro-meteorological impacts on crop production (Verdin and
44 Klaver, 2002).

45 *GeoWRSI*. Agencies concerned with drought monitoring and famine early
46 warning, including FEWS NET, have increasingly moved toward grid-based
47 use of WRSI, largely facilitated by the greater availability of gridded input
48 data on rainfall and reference, or potential, evapotranspiration (PET) (Senay
49 and Verdin, 2002, 2003; Verdin and Klaver, 2002). In 2002/03, FEWS NET
50 set up the geospatial (gridded) version of WRSI, GeoWRSI (Magadzire 2009
51 in Jayanthi et al. 2014), for **operational crop monitoring and yield esti-**
52 **mation** in 20 African countries, as well as in Central America, the Caribbean
53 (Haiti), Central Asia, and the Middle East (Afgahnistan) with daily and
54 dekadal outputs posted online at <http://earlywarning.usgs.gov/adds> (Verdin
55 and Klaver, 2002; Melesse et al., 2007; Shukla et al., 2014). Unlike the WRSI
56 in FAO’s Agrometshell software, GeoWRSI calculates water balance compo-
57 nents on a grid-cell basis (Jayanthi et al., 2014). GeoWRSI uses satellite-
58 based rainfall estimates, a potential evapotranspiration (PET) climatology
59 derived using the Penman-Monteith equation, soil water holding capacity
60 from digital soil databases, and published crop coefficient values (Kc) (Jayan-
61 thi and Husak, 2013).

62 Drought-related crop yield losses in response to water stress (rainfall
63 and/or soil moisture deficit) were successfully assessed for maize in Kenya,
64 Malawi, and Mozambique, and for millet in Niger through end-of-season
65 WRSI, the ratio of seasonal crop actual evapotranspiration (AET) to sea-

sonal crop water requirements, as an agricultural hazard index (Jayanthi et al., 2014). With the increasing availability of 30⁺ years satellite-based rainfall datasets, GeoWRSI has been used to produce probabilistic estimates of rainfall-driven yield variations. For example, a novel **probabilistic drought risk management** approach, considering the hazard, exposure, vulnerability, and risk components of agricultural drought risk profiling has helped to improve the statistical representation of hazards and risk exposures (Jayanthi et al., 2014). Alongside hydrologic and water balance models Noah and VIC, and other land surface models, WRSI is used in a **multi-model framework for seasonal agricultural drought forecasting** within the NASA FEWS NET Land Data Assimilation System (Shukla et al., 2014).

Previous Evaluations and Sensitivity Analysis. Although WRSI is widely used for operational crop performance monitoring, probabilistic drought risk management, and multi-model seasonal drought forecasting, a comprehensive absolute evaluation of WRSI relative to reported yield has not been carried out in many African countries, likely due to scarcity, or lack of, reliable agricultural statistics on crop yield, planted area, and seasonal production (Senay and Verdin, 2002, 2003). An overview of previous evaluations is given in Table 1. Regression correlations of WRSI with reported yields in the order of 0.75 are commonly reported (see references in Verdin and Klaver 2002), although these are usually for sub-national level and cover a time span between a single growing season and up to 10 years in one study.

Sensitivity of WRSI to inputs has been evaluated with the FAOINDEX

Table 1: Evaluations of WRSI against reported yield

Country (Crop)	Findings (References)
Ethiopia (sorghum)	Evaluated WRSI vs reported yield; district groups; 4 years (1996-1999); $R^2=0.77$ for years with WRSI below 98% (Senay and Verdin, 2002)
Ethiopia (maize)	Evaluated WRSI vs reported yield; 175 districts; 4 years (1996-1999); $R^2=0.92$ (Senay and Verdin, 2003)
Southern Africa (maize)	Higher correlation when yield reduction function considers long-term local average yield; 206 points; $R^2=0.86$ (Mattei and Sakamoto 1993 in Verdin and Klaver 2002)
Zimbabwe (maize)	Evaluated WRSI vs reported yield; 14 communal lands; 1996/97 season; $R^2=0.8$ (Verdin and Klaver, 2002)
India (maize, sorghum, pearl millet)	Evaluated WRSI vs reported yield; 7 years (1998-2004); mean significant $R^2=0.52$ (N=43); works well in drought-prone regions; higher R^2 for regions where proportion of area covered by each crop was higher; showed that drought stress can reduce season length by up to 20-30 days; observed declining trend in mean season length (Patel et al., 2011)
Kenya, Malawi, Mozambique (maize); Niger (millet)	WRSI used to develop crop yield loss functions (Jayanthi and Husak, 2013; Jayanthi et al., 2014); 10 years (2001-2010); $R^2=0.52$, 0.72, and 0.62 for Kenya, Malawi, and Mozambique, resp., and 0.64 for Niger

89 software (Gommes 1993 in Verdin and Klaver 2002) through simulations with
90 varying planting dekad or start of season (SOS), soil water holding capacity
91 (WHC), rainfall input, and PET. Results showed that $\pm 10\%$ change in rain-
92 fall or PET led to $\pm 5\%$ change in WRSI; similar sensitivity to shifting SOS
93 was observed, and WRSI varied substantially in response to WHC changes

94 with 25 mm and 50 mm increases leading to 10% and 16% increase of WRSI,
95 respectively ([Verdin and Klaver, 2002](#)).

96 *Motivation and Objectives.* Inherently, models such as WRSI depend to a
97 high degree on the quality of rainfall and reference evapotranspiration input
98 data. Rainfall validations and inter-comparisons focus on assessing the per-
99 formance of gridded rainfall data relative to point-based gauge observations
100 of rainfall. However, what matters most for crop water stress modelling and
101 weather index-based insurance products is the skill of rainfall datasets in cap-
102 turing agricultural drought parameters such as season onset, duration, and
103 cessation and the correlations between indicators such as WRSI with yield.

104 For example, in a West Africa study of rainfed cereal crops, [Ramarohetra](#)
105 [et al. \(2013\)](#) showed that the choice of rainfall product – mainly via the prod-
106 uct’s skill in capturing seasonal rainfall total and distribution of wet days –
107 can introduce large biases in crop yield simulations with the mechanistic crop
108 growth models SARRA-H and EPIC. To our knowledge, a similarly compre-
109 hensive analysis of WRSI’s sensitivity to rainfall inputs from different sources
110 has not been carried out. Thus, the objective here is to evaluate the sensitiv-
111 ity of WRSI to different rainfall datasets and crop variety parameterisations,
112 demonstrating the adapted WRSI developed here for a case study focused on
113 maize production in Tanzania. With this study we also extend to Tanzania
114 the evaluation of the WRSI method for assessing agro-meteorological risk on
115 maize production, and characterise the spatial and temporal variation in the
116 timing of the onset of rains and growing season duration defined using differ-

ent methods ([Senay and Verdin, 2003](#)). The outcomes of this will help inform weather index-based insurance design on the variability in the correlation of WRSI and reported yield for different rainfall inputs.

2. Study Region

The United Republic of Tanzania (hereafter Tanzania) (total area: approx. 947,300 m²; population: approx. 52 million) is situated on the eastern coast of Africa between 29-41°E and 1-12°S and has a diverse terrain with Africa's highest and lowest points, Mount Kilimanjaro (5,895 mASL) and the floor of Lake Tanganyika (352 mBSL), respectively.

Tanzania is dominated by tropical savanna, and warm semi-arid and arid climate zones. The eastern coastal region is hot and humid, while the high mountainous regions are cool. Mean annual temperatures in the highlands are between 10-20°C in the cold (May-August) and hot (November-February) seasons, respectively, and rarely fall below 20°C in the rest of the country.

Tanzania is characterised by two rainfall regimes. The unimodal zone in the central, southern, and western parts of the country has one main wet season 'Musumi' (October/November-April/May) prone to dry spells in February-April. The bimodal zone in the northeast mountainous region from Lake Victoria to the coast is defined by the seasonal north-south migration of the Inter-Tropical Convergence Zone (ITCZ) ([Zorita and Tilya, 2002](#)) with short 'Vuli' rains (October-November) and long 'Masika' rains (March-May).

Tanzania has diverse soils that are generally suitable for agricultural pro-

duction. However, physical soil loss through erosion and decline in soil fertility due to continuous cropping practices without replenishment of soil nutrients and minerals present major challenges for increasing crop yield.

Apart from large zones under wildlife and biodiversity protection, agriculture contributes to about a quarter of the gross domestic product, providing 85% of exports and employing over half of the workforce. Agricultural production is mainly rainfed with only 1% of agricultural land currently under irrigated farming. The largest food crop is maize with 1.5 Mha under maize production and 5.17 Mt production in 2013. Longer maize varieties are grown in the unimodal rainfall zone, while double harvest of shorter varieties is common in the bimodal rainfall zone.

3. Data and Modelling Approach

The WRSI/GeoWRSI model is described in [Senay and Verdin \(2003\)](#) among others and summarised in [Appendix A](#) along with its key advantages and disadvantages. In order to address some of the model's disadvantages and to enable testing of its sensitivity to rainfall inputs from different sources and different crop growing cycle parameterisations, we developed an adapted WRSI model described here.

3.1. The Adapted WRSI model

The adapted version of WRSI developed here allows for sensitivity analysis to rainfall with phenology-relevant metrics such as start of season (SOS),

length of the growing period (LGP), and end of season (EOS) through new capabilities to:

- drive the model with different rainfall input datasets,
- use a new, temporally-varying reference evapotranspiration input data, as opposed to climatological averages,
- use spatially-varying water holding capacity from a gridded soil database,
- apply different methods to define SOS and LGP, and
- calculate and output intra-seasonal variables such as cumulative rainfall at each crop development stage and seasonally, as well as water balance components such as soil moisture beyond the growing season.

3.1.1. Weather Data Inputs

Table 2 summarises the input reference evapotranspiration and rainfall data for the adapted WRSI model. Since the stochastic nature of climatic parameters plays a key role in the calculation of PET and AET, and subsequently WRSI and drought-related yield losses, using climatological PET values in WRSI may not be ideal (Kaboosi and Kaveh, 2010). Thus, we use a newly available, time-varying PET input dataset with each of three different rainfall data products (Table 2).

PET. Potential (reference) evapotranspiration (PET) data with the Penmann-Monteith equation (hereafter PET-PM) (Sperna Weiland et al., 2015) is available from the earth2Observe tier-1 forcing dataset at 0.5° resolution globally

Table 2: Model input data (PET-PM = Potential (reference) EvapoTranspiraton with Penman-Monteith equation; ARC2 = African Rainfall Climatology v2; CHIRPS = Climate Hazards group InfraRed Precipitation with Station data; TAMSAT = Tropical Applications of Meteorology using SATellite data and ground-based observations)

Dataset	Spatial Resolution	Time Step	Time Period
<i>Evapotranspiration</i>			
PET-PM	0.083°($\approx 8km$)	daily	1979 - 2014
<i>Rainfall</i>			
ARC2	0.10°($\approx 10km$)	daily	1983 - present
CHIRPS	0.05°($\approx 5km$)	pentad, dekadal, daily	1981 - present
TAMSAT	0.0375°($\approx 4km$)	dekadal, daily	1983 - present

181 (Schellekens et al., 2016). Here, we use a downscaled PET-PM dataset at
182 0.083° resolution from the same source (PML, 2017), providing daily refer-
183 ence evaporation values in kg m⁻² from 1979 to 2014 inclusive. The daily
184 data were aggregated to dekadal time to drive WRSI calculations.

185 *ARC2*. The NOAA African Rainfall Climatology (ARC) Version 2 dataset
186 (hereafter ARC2) (Novella and Thiaw, 2013) merges global precipitation
187 index (GPI) information (3-hourly infrared data) with quality-controlled
188 Global Telecommunication Systems (GTS) gauge observations of daily rain-
189 fall to provide daily rainfall estimates over Africa from 1983 to present. ARC2
190 is found to be consistent with two other satellite-based rainfall products,
191 GPCP v2.2 and CMAP, with correlations of 0.86 over a 27-year overlap time
192 period (Novella and Thiaw, 2013; Manzananas et al., 2014) and performed well
193 for estimation of seasonal rainfall totals (Diem et al., 2014). ARC2 is also

194 used for the R4 index based insurance in Ethiopia ([Sharoff et al., 2015](#)) and
195 in Africa Risk Capacity’s ARV software ([ARC, 2017](#)). The daily ARC2 data
196 ([NOAA-CPC, 2017](#)) were aggregated to dekadal time step.

197 *CHIRPS*. CHIRPS (Climate Hazards Group InfraRed Precipitation with
198 Station data) is an operational 35⁺ years quasi-global rainfall dataset devel-
199 oped by the University of California, Santa Barbara ([Funk et al., 2015](#)). The
200 data covers areas globally between 50°S-50°N from 1981 to the near-present,
201 and incorporates 0.05° satellite imagery with *in situ* station data to create
202 gridded rainfall time series for trend analysis and seasonal drought monitor-
203 ing. The CHIRPS version 2.0 final product provides information on daily and
204 pentad (5-daily) rainfall. In addition to gauge data from GTS, CHIRPS-final
205 uses all available sources of ground observations (such as GHCN, SASSCAL,
206 SWALIM, etc.) at both the pentad and monthly time step with pentads
207 re-scaled to match the monthly total. CHIRPS-final is generated once per
208 month (in the third week of the month for the preceding month) as some
209 station data are only available at the monthly time step. Daily CHIRPS
210 data ([UCSB-CHG, 2017](#)) were aggregated to dekadal time step.

211 *TAMSAT*. The TAMSAT (Tropical Applications of Meteorology using SATel-
212 lite and other data) research group at the University of Reading provides
213 satellite-based rainfall estimates for the African continent and Madagascar in
214 delayed near-real time. The TAMSAT rainfall estimation algorithm uses 15-
215 min (30-min prior to June 2006) infrared imagery from the Meteosat geosta-

tionary satellites and a climatology-based calibration relationships (varying regionally and monthly) derived from a proprietary gauge dataset and historical gauge-satellite data (Maidment et al., 2014; Tarnavsky et al., 2014). The TAMSAT v3 daily rainfall estimates (TAMSAT, 2017), disaggregated from the pentad time step using cold cloud duration information (Maidment et al., 2017), were aggregated to dekadal time step for the analysis here.

3.1.2. Soil and Crop Parameters

Soil Data. The Harmonized World Soil Database (HWSD) combines information from existing regional and national updates of soil information worldwide with the 1:5,000,000 scale FAO-UNESCO Soil Map of the World (FAO, 1971-1981) and contains over 15,000 different soil mapping units at 30 arc-second spatial resolution (FAO/IIASA/ISRIC/ISS-CAS/JRC, 2009a). Available water storage capacity ranging between 0-150 mm m⁻¹ (estimated according to FAO procedures accounting for topsoil textural class and depth/volume limiting soil phases) from the HWSD v1.2 dataset (FAO/IIASA/ISRIC/ISS-CAS/JRC, 2009b) is used to define spatially-varying water holding capacity (WHC) in the adapted WRSI model.

Crop Coefficients (Kc). Kc values provided by FAO are generally based on four crop growth stages: early (initial), vegetative (crop development), maturity (mid-season), and senescence (late season) where the early and mature stages are constant functions of time, and the vegetative and senescence stages are linear functions of time (Senay, 2008). Here, we use four-stage

238 K_c values for maize (*Zea mays* L.) (Steduto et al., 2012; Senay and Verdin,
239 2003) defined by 0.3, 1.2, and 0.35 at the early to vegetative, maturity to
240 senescence, and harvest stages respectively (Allen et al., 1998).

241 *Seasonal Parameters.* The adapted WRSI model allows for definition of the
242 start of season (SOS) from an external source or from rainfall input data using
243 the AGHRYMET threshold approach of a given dekad with 25 mm rainfall
244 followed by two dekads with 20 mm total rainfall as in the standard WRSI
245 (see Appendix A). Although the AGHRYMET approach for SOS definition
246 was developed for West Africa, Verdin and Klaver (2002) compared SOS
247 detected by WRSI with field reports for the 1996/97 and 1997/98 growing
248 seasons and showed that it is applicable for countries in southern Africa.

249 The length of the growing period (LGP) in the adapted WRSI can ei-
250 ther be set as a constant, typically 80-180 days (e.g. 90 days for short-cycle
251 maize, 160-days for long-cycle maize) or LGP can be defined from the per-
252 sistence of rainfall over reference evapotranspiration, i.e. the length of time
253 precipitation exceeds half of reference evapotranspiration as in the standard
254 WRSI/GeoWRSI (see Appendix A). Since the adapted WRSI uses time-
255 varying PET instead of climatology, LGP defined on the basis of rainfall
256 persistence over PET varies from year to year. Specifically, LGP for each
257 year is calculated from the SOS dekad while mean dekadal rainfall exceeds
258 half of mean dekadal PET within the current LGP, or until there are six con-
259 secutive dekads without rainfall, indicating end of season. Using the average
260 dekadal rainfall and PET within the current LGP allows for short dry spells

261 to occur.

262 With either method for SOS and LGP definition, the end of season (EOS)
263 is calculated as the sum of SOS and LGP in terms of dekad of the year (where
264 1-10 January is dekad 1 and 21-31 December is dekad 36).

265 Seasonal parameters are important, because crop variety and growing
266 cycle length impact on the attainable yield with short-cycle crops sensitive
267 to dry periods and long-cycle crops – to early EOS (Ramarohetra et al.,
268 2013). Thus, with the adapted WRSI model we characterise and quantify
269 the impact of seasonal parameters on WRSI as an indicator of crop yield.

270 3.2. Evaluation Data

271 For evaluation of WRSI simulations, we obtained yield data from the
272 Statistics Unit of the Tanzanian Ministry of Agriculture Livestock and Fish-
273 eries (MALF) (<http://www.kilimo.go.tz/>). The data covers the time period
274 between 1996 and 2009; however, from 2002 onwards, figures are reported for
275 several new districts and contain estimates from national agricultural census
276 for some years. Thus, only yield over the 1996-2002 time period is considered
277 in the evaluation.

278 3.3. Model simulations and evaluation of sensitivity to rainfall

279 Here we describe the WRSI simulation scenarios and present the approach
280 for evaluation of the model simulations.

281 3.3.1. *Simulations*

282 The adapted WRSI model, implemented in a spatially distributed mode,
283 was applied for a total of 15 simulations, 5 model runs with each of the three
284 rainfall data inputs and SOS identified using the WRSI threshold method.
285 For model runs with each rainfall input dataset, simulations 1-4 use a con-
286 stant LGP every season of 90, 120, 140, and 160 days, respectively, and
287 simulation 5 uses LGP, which varies from year to year as it is defined using
288 the WRSI approach based on rainfall persistence over time-varying PET.

289 The WRSI simulations cover the overlap time period between the rainfall
290 and evapotranspiration input datasets, i.e. 1983-2014 for WRSI simulations
291 with ARC2 and TAMSAT and 1981-2014 for those with CHIRPS rainfall
292 input dataset. For all WRSI simulations, soil moisture was initialised as half
293 of WHC after preliminary tests with values from dry soil to water at WHC
294 showed little effect on the results. WRSI simulations were applied only to
295 maize growing areas as of 2000 ([You and Wood, 2006](#)) and the evaluation
296 against reported yield was carried out only for these areas at country level.

297 3.3.2. *Evaluation*

298 The evaluation of the impact of different rainfall input datasets on WRSI
299 model simulations is carried out in three distinct parts.

300 The first part of the evaluation is focused on seasonal rainfall characteris-
301 tics to support the identification of areas that are likely to experience similar
302 agro-meteorological risk. Specifically, we evaluate the spatial patterns and

303 temporal trends of SOS, LGP, and EOS across model simulations and relative
304 to reported information on these.

305 In the second part, we examine the impact of different rainfall input
306 datasets on the detection of WRSI below 80% spatially and over time (in-
307 terpreted as below average crop production conditions). This is evaluated
308 relatively among the three rainfall input datasets, as well as in relation to
309 the five LGP scenarios (i.e. simulations 1-4 with 90, 120, 140, and 160 days
310 fixed LGP and simulation 5 with variable LGP using the WRSI method).

311 Last, we assess the relationship of simulated seasonal WRSI and histor-
312 ically reported maize yield at the country level. As in previously reported
313 comparisons (Table 1), seasonal WRSI values, as well as seasonal rainfall
314 and median soil moisture for dekads in the season, over pixels in the maize
315 growing areas (You and Wood, 2006) are averaged and compared through
316 linear regression to reported national yield figures.

317 4. Results and Discussion

318 Here we present the results from the evaluation of rainfall seasonality,
319 sensitivity of WRSI to rainfall input data, and correlations of WRSI, seasonal
320 rainfall, and median soil moisture with reported yield for maize in Tanzania.

321 4.1. Evaluation of rainfall seasonality

322 Using the adapted WRSI model, we applied the standard rainfall thresh-
323 old approach for SOS detection and the persistence of rainfall over evapo-
324 transpiration method for LGP determination to examine the spatial patterns

325 and trends in the timing of SOS, the duration of LGP, and subsequently, the
326 pattern and timing of EOS. It is worth noting that the focus is here on the
327 main rainy season in the unimodal zone as capturing the two shorter rainfall
328 seasons requires the use of two consecutive, and likely different, thresholds
329 for SOS detection within the same agronomic year.

330 Figure 1 illustrates the differences in the spatial pattern of SOS, LGP,
331 and EOS averaged over the time period covered by each rainfall product.

332 In the unimodal rainfall zone of Tanzania, the spatial patterns of SOS
333 in ARC2, CHIRPS, and TAMSAT are similar, albeit with an earlier season
334 onset in the ARC2 product on average across the country (dekad 28 corre-
335 sponding to the first dekad of October, $SD = 10.2$) than in CHIRPS and
336 TAMSAT (dekad 30 corresponding to dekad 3 of October with $SD = 7.6$ and
337 7.2 , respectively).

338 With respect to LGP, the ARC2 product shows some artefacts likely
339 due to the near-real time gauge-merging routine employed by the rainfall
340 estimation algorithm (Novella and Thiaw, 2013) and results in an average
341 LGP across the country of 14 dekads ($SD = 3.1$). CHIRPS reasonably well
342 captures on average across the country a growing season of 15 dekads ($SD =$
343 2.6), which corresponds to the typical season length from October/November
344 to April/May, and average LGP calculated from the TAMSAT product is 14.5
345 dekads ($SD = 2.8$).

346 As EOS is calculated by adding LGP to SOS, the spatial pattern of EOS
347 reflects the above discussion with simulations using CHIRPS as input rain-

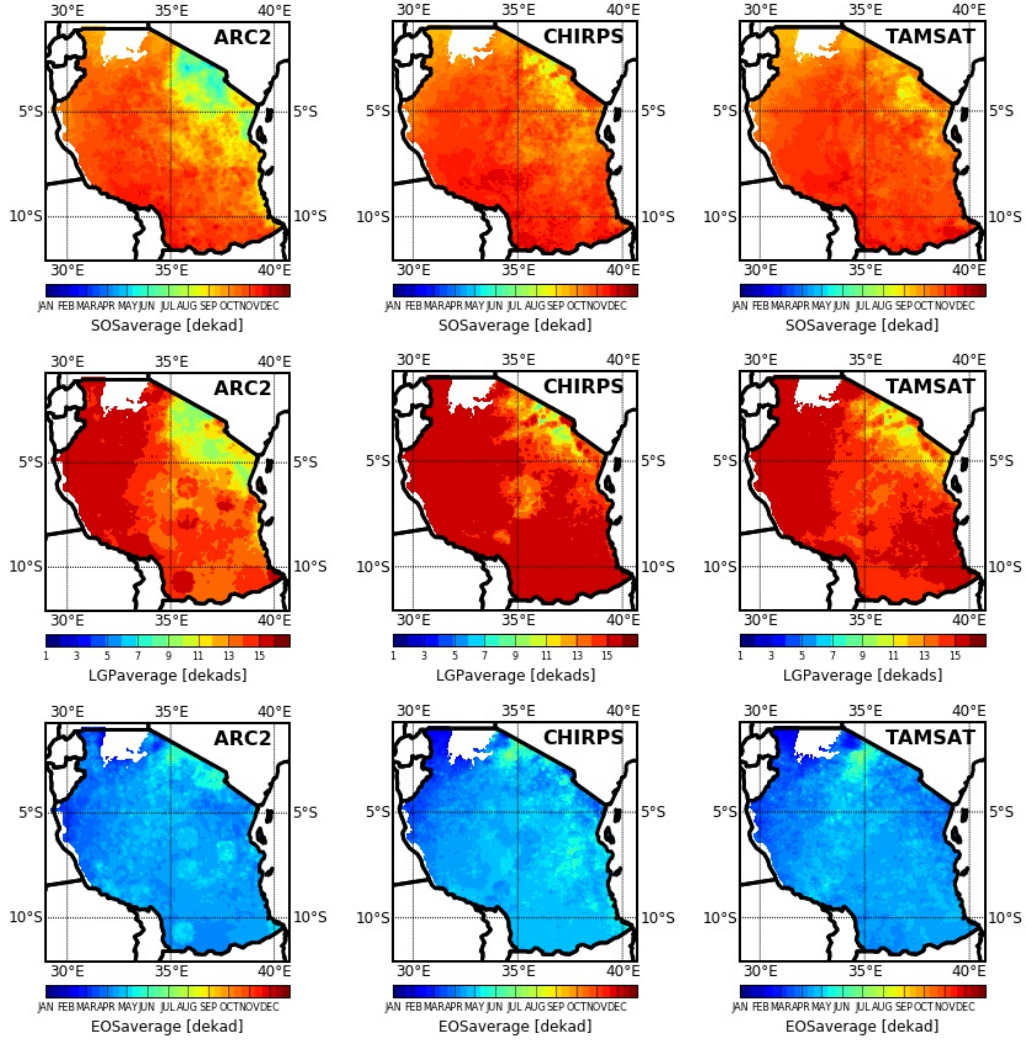


Figure 1: Average start of season (SOS) dekad determined using the WRSI rainfall threshold method (top), average length of growing period (LGP) defined using the WRSI method of rainfall ≥ 0.5 PET (middle), and average end of season (EOS) dekad (bottom) determined from the ARC2 (1983-2014), CHIRPS (1981-2014), and TAMSAT (1983-2014) rainfall products. Note: Inland water areas (Victoria, Tanganyika, and Nyasa lakes) are masked out.

348 fall data enabling to estimate the EOS reasonably well, i.e. on average in
 349 April/May. The spatial pattern of EOS also reflects the impact of artefacts

350 in the ARC2 product discussed above, as well as the slightly earlier SOS and
351 shorter LGP estimated by the ARC2 and TAMSAT products, as compared
352 to the SOS and LGP estimated with the CHIRPS product.

353 Figure 2 illustrates the averaged across the country SOS, LGP, and EOS
354 values over time as determined from the ARC2, CHIRPS, and TAMSAT
355 rainfall products. Overall, ARC2 shows the lowest mean SOS dekad (dekad
356 28-29 corresponding to dekads 1-2 of October) and highest variability over
357 time ($SD = 3.6$). For CHIRPS and TAMSAT these are dekad 30 (correspond-
358 ing to dekad 3 of October) with SD of 2.8 and 2.7 respectively. With regard
359 to LGP, CHIRPS shows the longest LGP of 15 dekads and the lowest SD of
360 0.6. For TAMSAT and ARC2 these are respectively LGP of 13.9 and 14.5
361 dekads with SD of 0.8 and 1.0. In terms of EOS, the variability is much less
362 substantial with all rainfall input datasets producing average EOS around
363 dekad 11 (corresponding to dekad 2 in April) and SD of 0.8, 0.9, and 1.0 for
364 ARC2, CHIRPS, and TAMSAT, respectively.

365 The above analysis shows the relative differences between the skill of
366 the three rainfall products in capturing the onset of rains, estimating the
367 length and subsequently, the end of the growing season. The variability of
368 SOS, LGP, and EOS detection has important implications for estimation of
369 seasonal WRSI and subsequently, for crop yield monitoring and forecasting
370 and agro-meteorological risk analysis on the basis of the WRSI model.

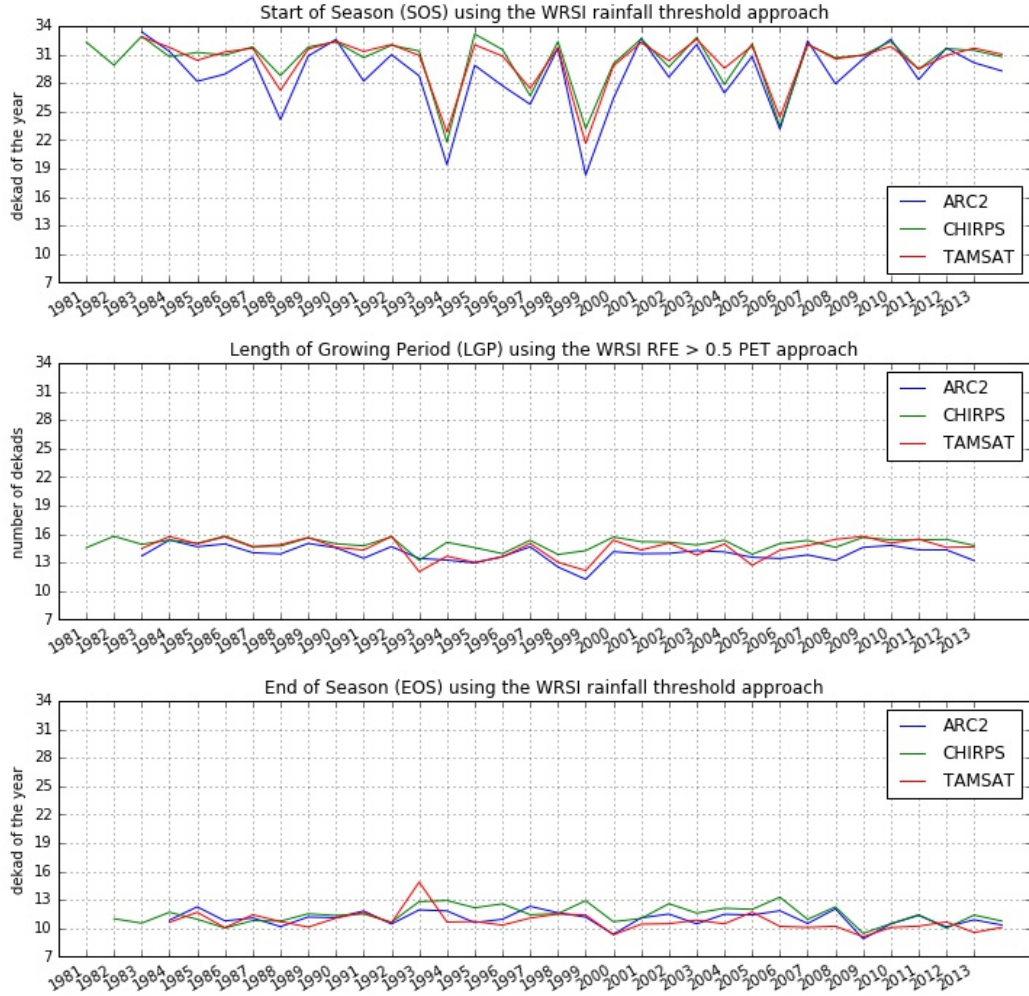


Figure 2: Regionally averaged start of season (SOS) determined using the WRSI rainfall threshold method, length of growing period (LGP) defined using the WRSI method of rainfall ≥ 0.5 PET, and end of season (EOS) determined from the ARC2, CHIRPS, and TAMSAT rainfall products.

371 4.2. Evaluation of WRSI sensitivity to rainfall inputs

372 Figure 3 shows the spatial pattern of average seasonal WRSI calculated
 373 with the standard WRSI approach for start of season based on rainfall thresh-
 374 old and the length of the growing period (LGP) defined on the basis of the
 375 persistence of rainfall over evapotranspiration. Across maize growing areas
 376 (You and Wood, 2006), for the unimodal zone similar average WRSI was
 377 calculated from simulations with ARC2 (1983-2014), CHIRPS (1981-2014),
 378 and TAMSAT (1983-2014). Average WRSI values over time from the simu-
 379 lations with all three rainfall data inputs are above 80%, indicating that on
 380 average the moisture requirements of maize are sufficiently met by available
 381 water. WRSI values fall below 80% for parts of the bimodal rainfall zone;
 382 however, this is not discussed as the adapted model cannot in its present
 383 form represent two short rainfall seasons within the same agronomic year.

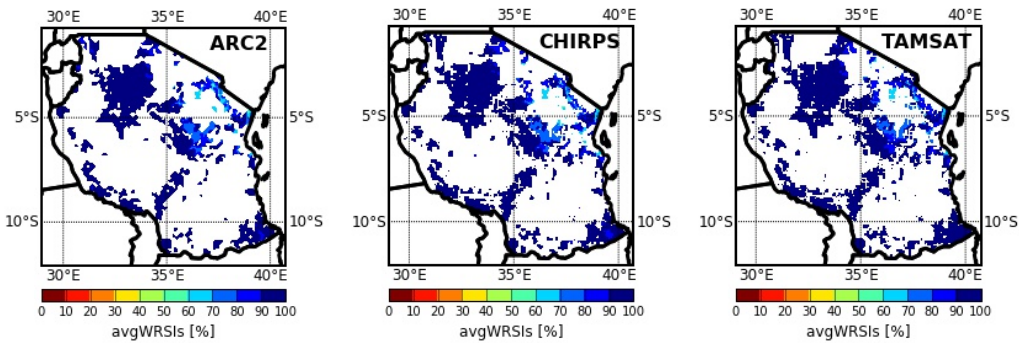


Figure 3: Average seasonal Water Requirements Satisfaction Index (WRSI) with the WRSI method for start of season (SOS) detection based on a rainfall threshold and length of growing period (LGP) defined as the length of time that rainfall ≥ 0.5 PET from the ARC2, CHIRPS, and TAMSAT rainfall products. Note: Areas not under maize production as of 2000 (You and Wood, 2006) are masked out.

Figure 4 illustrates the impact of rainfall input data on seasonal WRSI under the four scenarios of fixed length of the growing period (i.e. 90, 120, 140, and 160 days) and the scenario, under which LGP varies as a function of the persistence of rainfall over evapotranspiration. This results in lower variability over time of WRSI simulations with CHIRPS rainfall input and no years detected of regionally-averaged WRSI below 80% when CHIRPS and TAMSAT are used as rainfall input to WRSI simulations, while for ARC2 WRSI is below 80% for 160 days LGP in 1998 and 1999, and for 120, 140, and 160 days LGP in 1998, due to the earlier SOS and shorter LGP detected by ARC2. Overall, WRSI estimates based on CHIRPS and TAMSAT rainfall input data are higher than those with the ARC2 product. ARC2 based WRSI simulations also show the widest variation in standard deviation (SD) and CV respectively between 2.9 and 3% for the 90-days growing length simulation and 5.4 and 6% for the 160-days growing length simulation. CHIRPS based WRSI simulations result in the lowest SD and CV of 3.0 and 3% for the 90-days and WRSI method growing length scenarios and 4.0 and 4% for the 120-160 days growing length scenarios. WRSI results with TAMSAT as the rainfall input dataset are similar to those with CHIRPS, although less variable with SD and CV of 3.4 and 4% for the 90-days and WRSI method growing length scenarios and 4.8 and 5% for the 120-160 days growing length scenarios.

Table 3 shows the average total seasonal rainfall and WRSI using the ARC2, CHIRPS, and TAMSAT rainfall input datasets as an indication of

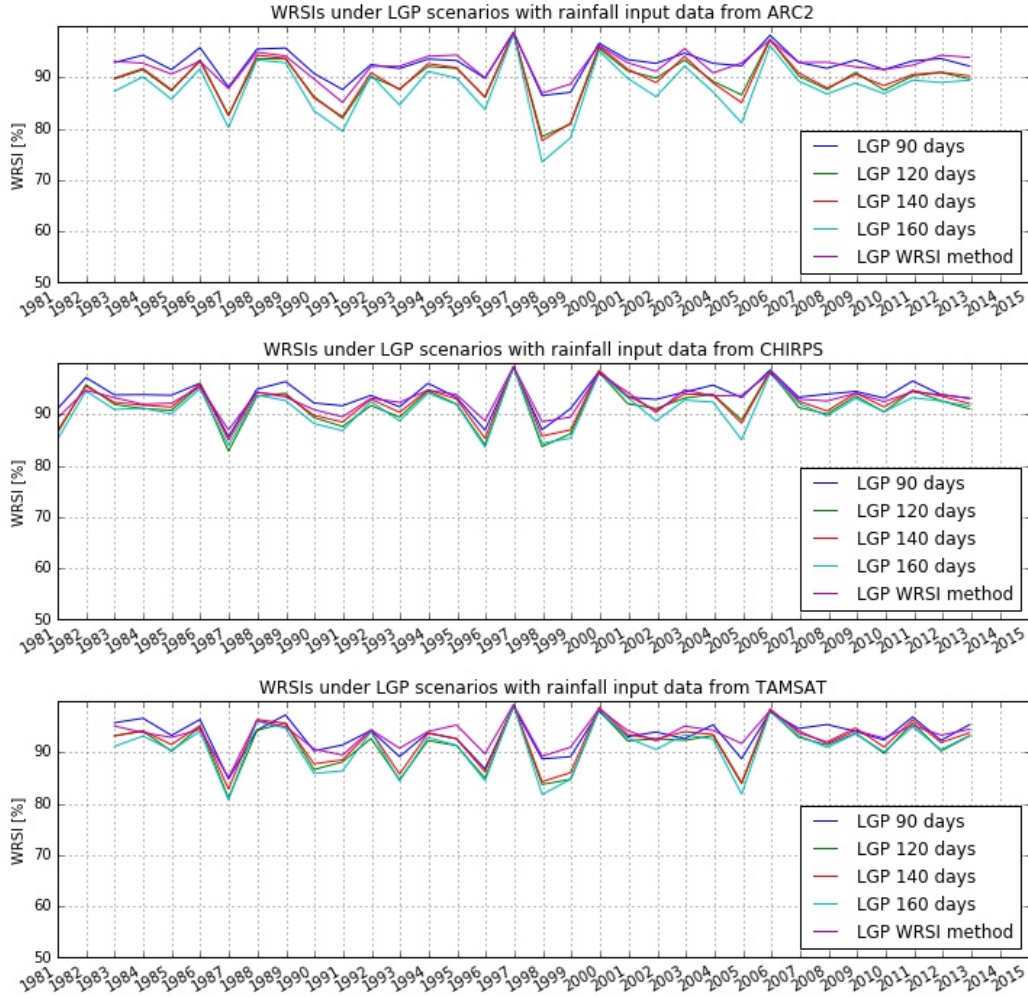


Figure 4: Regionally averaged WRSI defined with fixed length of the growing period (LGP) and using the WRSI method of rainfall ≥ 0.5 PET from the ARC2, CHIRPS, and TAMSAT rainfall products. Note: Inland water areas (Victoria, Tanganyika, and Nyasa lakes) are masked out, as well as areas not under maize production as of 2000 (You and Wood, 2006).

407 their skill in detecting the two years with lowest yield, i.e. 1996 and 1998
 408 with 1.07 and 1.06 t ha⁻¹, respectively. Using either indicator, only CHIRPS
 409 detects both 1996 and 1999 as low-yield years, although due to spatial and

temporal averaging all WRSI values are above 80%, indicating 'normal' (average) season conditions. It is worth noting that while both total seasonal rainfall and WRSI are lowest for ARC2 and TAMSAT, and WRSI is lowest for CHIRPS in 1998, it was a relatively high-yielding year. This suggests the inadequacy of basing agricultural drought insurance on rainfall indices alone and the need to analyse additional information from a crop water stress model such as WRSI. Moreover, the correlation between low-yield years and low rainfall in particular, but also low WRSI, can break down due to factors not related to rainfall and/or not represented in the WRSI model such as changes in nutrient input or acreage planted with maize from year to year.

Table 3: Skill of detection of low-yield years in the 1996-2002 time period assessed using total seasonal rainfall from the ARC2, CHIRPS, and TAMSAT rainfall products and using these as input, the simulated WRSI with varying length of the growing period (LGP). Note: Two lowest values in bold font

Year	Yield [t ha ⁻¹]	Rainfall [mm]			WRSI [%]		
		ARC2	CHIRPS	TAMSAT	ARC2	CHIRPS	TAMSAT
1996	1.07	493	459	495	90	89	90
1997	1.19	597	869	753	99	99	99
1998	1.33	377	530	473	87	89	89
1999	1.06	388	490	506	89	89	91
2000	1.71	575	647	658	96	98	98
2001	1.46	536	632	625	93	94	94
2002	1.15	491	544	520	91	90	92

420 *4.3. Evaluation of WRSI against yield at country level*

421 Correlations from the regression analysis of WRSI, total seasonal rainfall,
 422 and median soil moisture (Median SMs) and reported yield figures for 1996-
 423 2002 are summarised in Table 4, although none had a significant p-value.

Table 4: Correlations between Water Requirements Satisfaction Index (WRSI), total seasonal rainfall, and median soil moisture (Median SMs) and yield data (1996-2002) from the Tanzanian Ministry of Agriculture, Livestock and Fisheries (MALF) across maize growing areas. WRSI simulations 1-4 use fixed length of the growing period (LGP) of 90, 120, 140, and 160 days, and simulation 5 uses variable LGP defined from the persistence of rainfall over evapotranspiration. Bold figures indicate highest correlation for each LGP scenario; underlined figures indicate highest correlation for each input rainfall dataset; no values are significant at $p \leq 0.05$

Product	SIM1 LGP-90	SIM2 LGP-120	SIM3 LGP-140	SIM4 LGP-160	SIM5 WRSI
WRSI vs Yield [t/ha]					
ARC2	0.42	0.40	0.41	<u>0.45</u>	0.40
CHIRPS	0.47	0.52	0.57	<u>0.61</u>	0.56
TAMSAT	0.52	0.51	0.52	0.52	<u>0.53</u>
Rainfall vs Yield [t/ha]					
ARC2	<u>0.47</u>	0.42	0.39	0.38	0.37
CHIRPS	0.31	0.30	0.33	0.31	<u>0.34</u>
TAMSAT	<u>0.49</u>	0.42	0.43	0.38	0.41
Median SMs vs Yield [t/ha]					
ARC2	0.26	0.30	0.33	0.36	<u>0.38</u>
CHIRPS	0.38	0.46	0.52	0.53	<u>0.55</u>
TAMSAT	0.44	0.46	0.48	0.48	<u>0.58</u>

424 For WRSI simulations using the ARC2 rainfall input dataset, correla-
 425 tions between WRSI and yield were lowest ($R^2 < 0.5$) likely due to the earlier
 426 SOS and shorter LGP detected with the use of ARC2. This suggests that if
 427 ARC2 rainfall represents more realistically the spatial and temporal patterns

of rainfall, its performance in WRSI can be improved to reflect more closely reported yield even when results are averaged across a country such as Tanzania with two distinct rainfall zones. The CHIRPS rainfall input dataset produced WRSI estimates that most closely correlate with yield figures for all LGP scenarios except the 90-days simulation. Correlations between WRSI simulations with TAMSAT and yield were highest for the variable LGP and 90-days LGP scenarios.

The evaluation of seasonal total rainfall and median soil moisture (Median SMs) relative to historical yield figures shows overall lower correlations with rainfall explaining less than half of the yield variance in all simulations (Table 4). Median soil moisture explains only 26-38% of yield variance with the ARC2 rainfall data input, while 46-53% of yield variance is explained by rainfall when CHIRPS is used as input for all fixed LGPs except the 90-day scenario and 55% for the time-varying LGP scenario. Using TAMSAT as rainfall input data 58% of yield variance is explained only for the simulation with time-varying LGP. This suggests that CHIRPS is well suited for use in the WRSI model, likely due to the realistic representation of seasonally-varying phenology-relevant parameters such as SOS, LGP, and EOS.

The results from a 7-year evaluation of WRSI and reported yield over Tanzania presented here are consistent with previous evaluations that covered 7 years in India (Patel et al., 2011) and 10 years in Southern and Western African countries (Jayanthi and Husak, 2013; Jayanthi et al., 2014), especially for areas where rainfall is the main limiting factor. Even though the

451 area considered in the regression analysis includes parts of the bimodal zone
452 with two rainfall seasons in the northeast part of Tanzania, the correlations
453 achieved were similar to those reported in previous studies (see Table 1).

454 Discrepancies between simulated WRSI and other drought indicators and
455 yield are to be expected due to the high uncertainty of areas under maize
456 production in any given year historically, possibly a less stable acreage under
457 maize production over the years considered here, and/or the limited 7-year
458 historical production figures with sufficient reliability for analysis. It is worth
459 noting that the aim of the evaluation of WRSI against yield is not to repro-
460 duce accurately historical yields at country level, but to characterise the
461 impact of different rainfall datasets used as input to the WRSI model on
462 WRSI outcomes through the evaluation of key dynamic modelling parame-
463 ters such as season onset, cessation, and length of the growing period. This
464 is important particularly where the ARC2, CHIRPS or TAMSAT rainfall
465 datasets and WRSI are used as agro-meteorological risk and/or hazard indi-
466 cators such as in weather index-based insurance and risk profiling frameworks
467 based on statistical analysis of hazard, exposure, vulnerability, and risk.

468 Consistent with previous studies, some of the general challenges for histor-
469 ical validation of WRSI against reported yield include (i) staggered planting
470 which is difficult to reproduce historically, i.e. farmers plant maize and if it
471 fails, they plant sorghum, and if that fails, they may then re-plant with teff
472 (Senay and Verdin, 2003), (ii) low production in normal rainfall conditions
473 due to other factors such as floods, locust outbreaks, and nutrient inputs

474 that are not represented in WRSI (McNally et al., 2015), (iii) different vari-
 475 eties grown in different agro-ecological zones, while national average data and
 476 simulations across the country with a single LGP are not expected to repre-
 477 sent accurately the production/yield of mixed varieties, (iv) changes in crop
 478 management induced by government programmes (e.g. subsidised fertiliser),
 479 and (v) limited number of years with useable data after quality screening to
 480 detect outliers, and/or errors in historically reported figures of production-
 481 area-yield. The main challenge, however, is the uncertainty of reported area
 482 under maize production and changes in areas under maize production over
 483 time. Even though datasets on maize growing areas exist (You and Wood,
 484 2006), they provide a snapshot in time as an estimate and not actual, field-
 485 based information over time that can be used for an absolute validation.
 486 Specific to the evaluation of WRSI for Tanzania is the challenge of rainfall
 487 variability in the unimodal and bimodal zones, as well as the limited avail-
 488 ability of reliable long-term data on production-area-yield at sub-national
 489 level to distinguish between zones of unimodal and bimodal rainfall regimes.

490 5. Conclusions

491 We extended the evaluation of the WRSI method for assessing agro-
 492 meteorological risk such as drought on maize production through an adapted
 493 gridded version of the model and sensitivity analysis to rainfall inputs from
 494 three different sources, i.e. the ARC2, CHIRPS, and TAMSAT products.
 495 We characterised the spatial variation in the timing of the onset of rains and

496 analysed the impact of using different rainfall input datasets, as well as the
497 methods for definition of the start-of-season (SOS) and length of the growing
498 period (LGP) on WRSI outputs.

499 The analysis showed that the CHIRPS and TAMSAT rainfall input datasets
500 realistically represent season onset patterns, but CHIRPS performs best in
501 detecting SOS patterns and assessing the LGP, resulting in highest correla-
502 tions with WRSI. Understanding the impact of using different rainfall input
503 datasets in WRSI helps to identify regions that are likely to experience sim-
504 ilar agro-meteorological risks as relevant for the design and structure of risk
505 management instruments such as weather index-based insurance. As a mini-
506 mum, our results indicate that separate weather index-based insurance might
507 be appropriate for the unimodal and bimodal zones in Tanzania.

508 Through WRSI simulations, we explored water-stressed regions in the
509 maize growing area of Tanzania with other factors assumed constant (vari-
510 ety, fertiliser use, pests, diseases, etc.) and established the correlations be-
511 tween WRSI, seasonal rainfall, and median soil moisture and reported maize
512 yield at the national level. CHIRPS-based WRSI and median soil moisture
513 showed highest correlations with yield for the majority of simulations. This
514 is despite the limitation of our study in that the country-level analyses of
515 seasonality and WRSI response to different rainfall input datasets includes
516 areas in the bimodal zone of the country in the northeast along the bor-
517 der with Kenya, while in its present form the adapted WRSI model is not
518 set up to accommodate two short-duration rainfall seasons within the same

519 agronomic year.

520 The results of this work suggest that CHIRPS is better suited for ap-
521 plications in weather index-based insurance and early warning monitoring
522 with the WRSI model, while with ARC2 and TAMSAT the variability of the
523 correlations between rainfall and WRSI model outputs and reported yield
524 is greater and provides a less clear indication of their utility in structur-
525 ing weather indices. Further work is required to build in capability in the
526 WRSI model for representation of bimodal rainfall information so that the
527 adapted WRSI model can be used to identify regions of similar rainfall season
528 progression and climatology, and to account for the role of temperature in
529 defining the growing season. Sub-national validation is desirable, provided
530 the patterns of rainfall require higher spatial detail and reliable yield data are
531 available, preferably over a longer period. Investigations in this area can be
532 supported by analysis of the change of maize growing area over time. Overall,
533 this can support the defining of risk areas and applying of risk management
534 instruments accordingly.

535 **Acknowledgements** The authors acknowledge the WINnERS (Weather
536 INdex-based wEather-driven Risk Services) project funded by the Climate-
537 KIC initiative of the European Institute of Innovation Technology (EIT)
538 grant number 520000117. We are grateful to Dr Wei Xiong (International
539 Maize and Wheat Improvement Center (CIMMYT), Mexico) for providing
540 maize growing areas data developed by [You and Wood \(2006\)](#).

References

- Allen, R. G., Pereira, L. S., Raes, D., Smith, M., 1998. Crop evapotranspiration - Guidelines for computing crop water requirements - FAO Irrigation and drainage paper 56. Tech. rep., FAO, Rome, Italy.
- ARC, 2017. The Africa Risk Capacity (ARC) Africa RiskView (ARV) software.
- URL <http://www.africanriskcapacity.org/2016/10/31/africa-riskview-methodology/>
- Bastagli, F., Harman, L., 2015. The Role of Index-Based Triggers in Social Protection Shock Response. Tech. Rep. April, Overseas Development Institute (ODI), London, UK.
- Bryla, E., Syroka, J., mar 2007. Developing Index-Based Insurance for Agriculture in Developing Countries. Sustainable Development Innovation Briefs (2), 8.
- Crowther, E., 2007. Insuring disaster: A study of weather index-based insurance in developing world agriculture. Msc thesis, School of Oriental and African Studies, University of London.
- Diem, J. E., Hartter, J., Ryan, S. J., Palace, M. W., 2014. Validation of Satellite Rainfall Products for Western Uganda. Journal of Hydrometeorology 15 (5), 2030–2038.

561 FAO/IIASA/ISRIC/ISS-CAS/JRC, 2009a. Harmonized World Soil Database
 562 (HWSD) Version 1.1. Tech. rep., FAO/IIASA/ISRIC/ISS-CAS/JRC2009.
 563 URL [http://webarchive.iiasa.ac.at/Research/LUC/](http://webarchive.iiasa.ac.at/Research/LUC/External-World-soil-database/HTML/index.html?sb=1)
 564 [External-World-soil-database/HTML/index.html?sb=1](http://webarchive.iiasa.ac.at/Research/LUC/External-World-soil-database/HTML/index.html?sb=1)

565 FAO/IIASA/ISRIC/ISS-CAS/JRC, 2009b. The Harmonized World Soil
 566 Database (HWSD) Version 1.2.
 567 URL [http://www.fao.org/soils-portal/soil-survey/](http://www.fao.org/soils-portal/soil-survey/soil-maps-and-databases/harmonized-world-soil-database-v12/en/)
 568 [soil-maps-and-databases/harmonized-world-soil-database-v12/en/](http://www.fao.org/soils-portal/soil-survey/soil-maps-and-databases/harmonized-world-soil-database-v12/en/)

569 Frere, M., Popov, G. F., 1979. Agrometeorological crop monitoring and fore-
 570 casting. Tech. rep., FAO, Rome, Italy.

571 Funk, C., Verdin, A., Michaelsen, J., Peterson, P., Pedreros, D., Husak, G.,
 572 2015. A Global Satellite-Assisted Precipitation Climatology. Earth System
 573 Science Data 7, 275–287.

574 Jayanthi, H., Husak, G., 2013. A probabilistic approach to assess agricultural
 575 drought risk.

576 Jayanthi, H., Husak, G. J., Funk, C., Magadzire, T., Adoum, A., Verdin,
 577 J. P., 2014. A probabilistic approach to assess agricultural drought risk to
 578 maize in Southern Africa and millet in Western Sahel using satellite esti-
 579 mated rainfall. International Journal of Disaster Risk Reduction 10 (PB),
 580 490–502.

581 Kaboosi, K., Kaveh, F., 2010. Sensitivity analysis of Doorenbos and Kassam
582 (1979) crop water production function. *African Journal of Agricultural*
583 *Research* 5 (17), 2399–2417.

584 Maidment, R. I., Grimes, D., Allan, R. P., Tarnavsky, E., Stringer, M.,
585 Hewison, T., Roebeling, R., Black, E., 2014. The 30 year TAMSAT African
586 Rainfall Climatology And Time Series (TARCAT) data set. *Journal of*
587 *Geophysical Research: Atmospheres* 119, 10619–10644.

588 Maidment, R. I., Grimes, D., Black, E., Tarnavsky, E., Young, M., Greatrex,
589 H., Allan, R. P., Stein, T., Nkonde, E., Senkunda, S., Misael, E., Alcántara,
590 U., 2017. Data Descriptor: A new, long-term daily satellite-based rainfall
591 dataset for operational monitoring in Africa. *Scientific Data* 4:170063, 1–
592 17.

593 Manzananas, R., Amekudzi, L. K., Preko, K., Herrera, S., Gutiérrez, J. M.,
594 2014. Precipitation variability and trends in Ghana: An intercomparison
595 of observational and reanalysis products. *Climatic Change* 124, 805–819.

596 McNally, A., Husak, G. J., Brown, M., Carroll, M., Funk, C., Yatheendradas,
597 S., Arsenault, K., Peters-Lidard, C., Verdin, J. P., 2015. Calculating Crop
598 Water Requirement Satisfaction in the West Africa Sahel with Remotely
599 Sensed Soil Moisture. *Journal of Hydrometeorology* 16 (1), 295–305.

600 Melesse, A. M., Weng, Q., Thenkabail, P. S., Senay, G. B., 2007. Remote

601 Sensing Sensors and Applications in Environmental Resources Mapping
602 and Modelling. *Sensors* 7 (12), 3209–3241.

603 NOAA-CPC, 2017. The NOAA African Rainfall Climatology (ARC) Version
604 2 dataset (ARC2).
605 URL <ftp://ftp.cpc.ncep.noaa.gov/fews/fewsdata/africa/arc2/geotiff/>

606 Novella, N. S., Thiaw, W. M., sep 2013. African Rainfall Climatology Version
607 2 for Famine Early Warning Systems. *Journal of Applied Meteorology and*
608 *Climatology* 52 (1996), 588–606.

609 Patel, N. R., Sarkar, M., Kumar, S., 2011. Use of earth observation for
610 geospatial crop water accounting of rain-fed agro-ecosystem in india. *Earth*
611 *Observation for Terrestrial Ecosystems XXXVIII* (November), 23–28.

612 PML, 2017. Reference Evapotranspiration Penman-Monteith.
613 URL [https://wci.earth2observe.eu/thredds/catalog/deltares/PET/wrr2/](https://wci.earth2observe.eu/thredds/catalog/deltares/PET/wrr2/0.083degree/penmanmonteith/catalog.html)
614 [0.083degree/penmanmonteith/catalog.html](https://wci.earth2observe.eu/thredds/catalog/deltares/PET/wrr2/0.083degree/penmanmonteith/catalog.html)

615 Ramarohetra, J., Sultan, B., Baron, C., Gaiser, T., Gosset, M., 2013. How
616 satellite rainfall estimate errors may impact rainfed cereal yield simulation
617 in West Africa. *Agricultural and Forest Meteorology* 180, 118–131.

618 Rojas, O., Rembold, F., Royer, A., Negre, T., 2005. Agronomy for sustainable
619 development. *Agronomy for Sustainable Development* 25, 63–77.

620 Schellekens, J., Dutra, E., Torre, A. M.-d., Balsamo, G., Van, A., Weiland,
621 F. S., Minvielle, M., Calvet, J.-c., Decharme, B., Eisner, S., Fink, G.,

- 622 Flörke, M., Peßenteiner, S., Beek, R. V., Polcher, J., Beck, H., Orth,
623 R., Calton, B., Burke, S., Dorigo, W., Weedon, G. P., 2016. A global
624 water resources ensemble of hydrological models: the earthH2Observe Tier-
625 1 dataset. *Earth Syst Sci Data Discuss* (December), 1–35.
- 626 Senay, G. B., 2008. Modeling landscape evapotranspiration by integrating
627 land surface phenology and a water balance algorithm. *Algorithms* 1 (2),
628 52–68.
- 629 Senay, G. B., Verdin, J., 2002. Evaluating the performance of a crop water
630 balance model in estimating regional crop production. In: *Proceedings of*
631 *the Pecora 15 Symposium*, Denver, CO. Denver, Colorado, USA, p. 8.
- 632 Senay, G. B., Verdin, J., 2003. Characterization of yield reduction in Ethiopia
633 using a GIS-based crop water balance model. *Canadian Journal of Remote*
634 *Sensing* 29 (6), 687–692.
- 635 Sharoff, J., Diro, R., Mccarney, G., Norton, M., 2015. R4 Rural Resilience
636 Initiative in Ethiopia. Tech. rep., Climate Services Partnership.
- 637 URL [http://www.climate-services.org/wp-content/uploads/2015/09/](http://www.climate-services.org/wp-content/uploads/2015/09/R4{-}Ethiopia{-}Case{-}Study.pdf)
638 [R4{-}Ethiopia{-}Case{-}Study.pdf](http://www.climate-services.org/wp-content/uploads/2015/09/R4{-}Ethiopia{-}Case{-}Study.pdf)
- 639 Shukla, S., McNally, A., Husak, G., Funk, C., 2014. A seasonal agricultural
640 drought forecast system for food-insecure regions of East Africa. *Hydrology*
641 *and Earth System Sciences Discussions* 11 (3), 3049–3081.

642 Sperna Weiland, F., Lopez, P., van Dijk, A., Schellekens, J., 2015. Global
643 high-resolution reference potential evaporation. In: 21st International
644 Congress on Modelling and Simulation. Gold Coast, Australia, pp. 2548–
645 2554.

646 Steduto, P., Hsiao, T. C., Fereres, E., Raes, D., 2012. Crop yield response to
647 water. Tech. rep., FAO, Rome, Italy.

648 TAMSAT, 2017. TAMSAT v3.
649 URL <http://www.tamsat.org.uk/public{ }data/TAMSAT3>

650 Tarnavsky, E., Grimes, D., Maidment, R., Black, E., Allan, R., Stringer, M.,
651 Chadwick, R., Kayitakire, F., 2014. Extension of the TAMSAT Satellite-
652 based Rainfall Monitoring over Africa and from 1983 to present. Journal
653 of Applied Meteorology and Climatology 53, 2805–2822.

654 UCSB-CHG, 2017. The Climate Hazards group InfraRed Precipitation with
655 Station data (CHIRPS).
656 URL <ftp://ftp.chg.ucsb.edu/pub/org/chg/products/CHIRPS-2.0>

657 Verdin, J., Klaver, R., 2002. Grid-cell-based crop water accounting for the
658 famine early warning system. Hydrological Processes 16 (8), 1617–1630.

659 You, L., Wood, S., 2006. An entropy approach to spatial disaggregation of
660 agricultural production. Agricultural Systems 90, 329–347.

661 Zorita, E., Tilya, F. F., 2002. Rainfall variability in Northern Tanzania in the

662 March–May season (long rains) and its links to large-scale climate forcing.
663 Climate Research 20, 31–40.

664 **Appendix A.**

665 **The Water Requirements Satisfaction Index (WRSI) Model**

666 WRSI requires as inputs information on rainfall and potential evapotranspi-
667 ration, as well as soil water holding capacity and crop coefficients to calculate
668 actual evapotranspiration, soil moisture, and WRSI during the crop growing
669 season. Calculations are carried out on dekadal time step as defined by the
670 World Meteorological Organisation (WMO), i.e. by dividing each month in
671 three dekads with dekad 1 from 1st to the 10th inclusive, dekad 2 from the
672 11th to the 20th inclusive, and dekad 3 for the remaining 8-11 days depending
673 on the month (WMO 1992 in [Verdin and Klaver 2002](#)). Since a daily time
674 step makes modelling data-intensive without a proportional gain in informa-
675 tion and a monthly time step fails to capture important vegetation growth
676 stages, the dekadal time step has proved useful for agro-meteorological mon-
677 itoring ([Verdin and Klaver, 2002](#)). Reference (potential) evapotranspiration,
678 hereafter referred to as PET, represents the water demand for crop growth.
679 Actual evapotranspiration (AET) is the actual soil water extracted used by
680 the crop from its root zone ([Jayanthi and Husak, 2013](#)).

681 The USGS GeoWRSI in FEWS NET uses the following input datasets:

- 682 • Dekadal satellite-based rainfall estimates from the NOAA CPC RFE2.0
683 dataset at 0.1° (~ 10 km) resolution ([Verdin and Klaver, 2002](#)).
- 684 • Dekadal PET at 1.0° (~ 100 km) calculated with the Penman-Monteith
685 equation (Shuttleworth 1992 in [Senay and Verdin 2002, 2003](#); [Verdin](#)

686 and Klaver 2002) from 6-hourly numerical meteorological model output
687 (Senay et al 2007b in Melesse et al. 2007, Verdin and Klaver 2002).

- 688 • Spatially varying soil information from FAO’s digital database and to-
689 pographical parameters from HYDRO-1K data based on Digital Ele-
690 vation Model (DEM) (FAO 1988 and Gesch et al 1999 in Senay and
691 Verdin 2002) or from the GTOPO30 DEM (Senay and Verdin, 2003).
- 692 • Crop coefficient values, varying throughout the growing season ob-
693 tained from the FAO online database at [http://www.fao.org/nr/water/](http://www.fao.org/nr/water/cropinfo_maize.html)
694 [cropinfo_maize.html](http://www.fao.org/nr/water/cropinfo_maize.html) (Jayanthi et al., 2014). For maize, Kc values are
695 given as 0.30, 0.30, 1.20, 1.20, and 0.35 for the times corresponding to
696 0, 16, 44, 76, and 100% of LGP, respectively (Senay and Verdin, 2003).

697 *Start of season (SOS)*. In WRSI, SOS for each pixel is defined, starting sev-
698 eral dekads before the typical SOS, by identifying a dekad with at least 25 mm
699 rainfall, followed by at least 20 mm rainfall total in the next two consecutive
700 dekads (Senay and Verdin, 2002; Verdin and Klaver, 2002) according to the
701 method defined by the Agriculture-Hydrology-Meteorology (AGHRYMET)
702 Regional Center in Niger (AGHRYMET 1996 in Verdin and Klaver 2002).
703 This method is used for monitoring with time-varying rainfall, although it
704 can be too strict for semi-arid areas (Senay 2004 available at [http://iridl.](http://iridl.ldeo.columbia.edu/documentation/usgs/adds/wrsi/WRSI_readme.pdf)
705 [ldeo.columbia.edu/documentation/usgs/adds/wrsi/WRSI_readme.pdf](http://iridl.ldeo.columbia.edu/documentation/usgs/adds/wrsi/WRSI_readme.pdf)). An
706 alternative SOS detection method in WRSI is when the ratio between av-
707 erage rainfall and PET is greater than 0.5 (McNally et al. 2015; Hare and

708 Oglallo 1993 and Mersha 2001 in Senay 2004), although justification for se-
709 lecting this threshold is not presented. This method is used with the cli-
710 matological CHARM-WRSI dataset (Funk et al 2003 in Senay 2004). In
711 WRSI, SOS indicates planting dates and triggers seasonal water balance cal-
712 culations. Since irregularities in SOS have substantial impacts on early crop
713 development (e.g. dry and hot conditions shorten the grain filling stage and
714 decrease expected yields), realistic and skilful SOS detection is critical for
715 successful crop performance monitoring.

716 *Length of growing period (LGP)*. In WRSI, similarly to one of the methods
717 for SOS detection, LGP is determined by the persistence, on average, above
718 a threshold value of a climatological ratio between rainfall and PET ([Senay
719 and Verdin, 2002](#)), i.e. crop growing period continues while average rainfall
720 exceeds half of average PET ([McNally et al., 2015](#)). Thus, LGP does not
721 vary year-to-year. Since WRSI values depend on the crop’s LGP, the ratio
722 of WRSI for current season over mean WRSI over the long-term is used as
723 an indicator of drought-related yield loss.

724 *End of season (EOS)*. EOS in WRSI is derived by adding LGP to SOS.
725 Hence, EOS varies as a function of SOS and over time for every location, e.g.
726 9 dekads in arid and semi-arid regions to 18 dekads in wetter and mountainous
727 regions ([Melesse et al., 2007](#)).

WRSI. End-of-season WRSI is computed as the ratio of supply, or demand
met (i.e. total crop water requirement satisfied by rainfall and available

moisture) and demand (i.e. seasonal crop water requirement) (Verdin and Klaver, 2002) with crop potential evapotranspiration (PETc) and seasonal crop actual evapotranspiration (AETc) expressed as percentage (Eq A.1). WRSI of 95-100% indicates no water deficit (i.e. adequate rainfall and moisture availability, or absence of yield reduction due to water deficit), values between 95% and 50% indicate varying degree of water stress and yield reduction due to inadequate water supply, and values below 50% indicate crop failure (Smith 1992 in Senay and Verdin 2002, 2003).

$$WRSI = \frac{\sum AET_c}{\sum PET_c} \times 100 \quad (A.1)$$

Where the crop water requirement PETc in [mm] is calculated at the dekadal time step during the growing season as follows:

$$PET_c = K_c \times PET \quad (A.2)$$

PAW. In order to determine AETc, the actual amount of water withdrawn from the soil profile, dekadal precipitation (PPT) is added to soil water (SW) to calculate plant-available water (PAW) (see Eq A.3) and this is compared to the value of critical soil water (SWC) (see Eq A.4).

$$PAW_d = SW_{d-1} + PPT_d \quad (A.3)$$

Soil Water Critical (SWC). Typically, for WHC somewhat arbitrary values such as 50 or 100 mm are used, esp. where reliable field data and digital soil maps are lacking (Verdin and Klaver, 2002). The operational FEWS NET WRSI version uses WHC for the top 100 cm from FAO digital soil map of the world (FAO 1994 in Verdin and Klaver 2002) to calculate SWC as follows:

$$SWC = WHC \times SW_f \times RD_f \quad (A.4)$$

728 Where WHC is water holding capacity of the soil, SW_f (0.45 for maize) is
 729 the fraction of WHC that defines the available soil water level, below which
 730 AET_c becomes less than PET_c, and RD_f is the root depth fraction, which
 731 ranges between 0 and 1, and equals 1 when the crop is mature.

AET_c. AET_c is determined according to Eq A.5 on the basis of the relationship between PAW and SWC.

$$AET_c = \begin{cases} PET_c, & PAW \geq SWC \\ \frac{PAW}{SWC} \times PET_c, & PAW < SWC \\ PAW, & AET_c > PAW \end{cases} \quad (A.5)$$

Soil Water (SW). The final soil water content at the end of simulation period (SW_d), is calculated as follows:

$$SW_d = \begin{cases} WHC, & SW_d > WHC \\ 0, & SW_d < 0.0 \\ SW_d = SW_{d-1} + PPT_d - AET_c, & otherwise \end{cases} \quad (A.6)$$

732 *Yield Reduction Response (Ky).* Similarly to Kc, Ky is crop- and location-
 733 dependent (Reynolds 1998 in [Senay and Verdin 2002](#)) with published values
 734 (FAO1996); for example, Ky of 0.9 for sorghum means that a 10% reduction
 735 of WRSI from the optimal 100 is related to a 9% reduction of sorghum yield.
 736 It is also worth noting that Ky values were established using high-yielding
 737 varieties and field experiments and further explanation of Ky, as well as
 738 references to published values, are available elsewhere ([Jayanthi and Husak,](#)
 739 [2013](#)). [Kaboosi and Kaveh \(2010\)](#) examined the sensitivity of the crop water
 740 production function to Ky, as well as PET and AET, and highlighted the
 741 importance of accurately defining crop growth stages (the length of which can
 742 be substantially different than those given by FAO 56 due to the diversity
 743 of crop varieties) and that high-yield varieties were more sensitive to water
 744 stress than low-yielding varieties.

745 **WRSI Advantages**

- 746 • Requires minimal data to initiate water budget processes and provides
 747 spatially continuous, near real-time info ([Verdin and Klaver, 2002](#))

- 748 • Can help identify crop production decline/failure well before agricul-
749 tural reports and statistics become available, i.e. several months after
750 harvest ([Verdin and Klaver, 2002](#)); Effectively estimates yield reduction
751 in dry years for drought-prone areas ([Senay and Verdin, 2002](#))
- 752 • Can serve as a proxy of crop yield, i.e. can be related to crop production
753 using a crop-specific linear yield reduction function (Doorenbos and
754 Pruitt 1977 in [Senay and Verdin 2002](#); [Jayanthi and Husak 2013](#))
- 755 • Captures well inter-annual and spatial variability of water availability
756 for crop production; good correlation with reported district-level yields,
757 esp. for drought-prone rainfed agricultural areas ([Patel et al., 2011](#))
- 758 • Captures impact of the timing of rainfall season, total seasonal rain-
759 fall, and seasonal rainfall distribution on crop yields (Syroka 2006 in
760 [Crowther 2007](#)) with the causal link between weather and crop yield
761 shortfall/loss being crucial for the success of index insurance schemes
- 762 • Tracks WRSI throughout the growing season, i.e. different role of rain-
763 fall deficit at the start of the season, and moisture deficits most critical
764 at the flowering and crop development stages, i.e. stunted crop growth,
765 reduced crop yield ([Jayanthi and Husak, 2013](#))
- 766 • As WRSI considers yield variability relative to water availability, where
767 WRSI is optimal, year-to-year variations can be attributed to other fac-
768 tors (heat stress, management practices, etc.), i.e. crop-specific effects

- 769 of non-water drivers of yield variability ([Senay and Verdin, 2002](#))
- 770 • Helps identify water-limited and water-unlimited areas for planning
 - 771 crops to be planted, e.g. high water requirements of maize, drought re-
 - 772 sistant sorghum, and flexible teff in Ethiopia ([Senay and Verdin, 2003](#))
 - 773 • Produces intermediate products that are useful in early warning and
 - 774 humanitarian aid planning/response, e.g. SOS map, soil water index
 - 775 (SWI) as a function/percentage of water holding capacity (WHC), spa-
 - 776 tial distribution of WRSI dekadal values, and dekadal anomalies in
 - 777 the form of observed (monitoring) and extended (forecasting) products
 - 778 ([Melesse et al., 2007](#))

779 **WRSI Disadvantages**

- 780 • Spatial resolution of 10-km limited by inputs means that the model
- 781 encompasses pixels containing different agro-ecological zones and more
- 782 than one crop by several thousand smallholder farmers ([Verdin and](#)
- 783 [Klaver, 2002](#))
- 784 • Model performance varies spatially, i.e. model not equally reliable
- 785 across large regions and continents
- 786 • High year-to-year variability of yield when WRSI is optimal ($\approx 100\%$)
- 787 is attributable to other, non-rainfall drivers ([Senay and Verdin, 2002](#))
- 788 • SOS defined from rainfall is limited by the skill of satellite rainfall
- 789 datasets, and thus by sparse rain gauge networks ([Patel et al., 2011](#))

- 790 • No indication of soil moisture outside growing season ([Senay, 2008](#))
- 791 • Use of Kc poses limitations: 1) Kc values are crop-specific, i.e. re-
792 quire prior knowledge of crop planted in the region; 2) Kc values are
793 region-specific, as crop growth is influenced by local climate, soils, etc;
794 3) requires knowledge of Kc values (or assumption of these) across the
795 crop calendar at each crop development stage: initial, vegetative, ma-
796 ture, senescence ([Senay, 2008](#)); 4) LGP with Kc (spatial) adjustment
797 does not work well for long growth cycle crops (e.g. sorghum); and 5)
798 Kc breaks down for sparse crops, i.e. under non-standard conditions
799 ([Senay 2008](#); Fig 2, p 32 in [Steduto et al. 2012](#))
- 800 • Calculations require WHC information as an arbitrary value (50-100
801 mm) or spatially-varying WHC from digital soil databases ([Verdin and](#)
802 [Klaver, 2002](#)); In the latter, the accuracy of water budget calculations
803 relies on WHC reflecting realistically field conditions
- 804 • Focused on water stress effects on crop production, while it would ben-
805 efit from information on heat stress, e.g. growing degree days (GDD)
806 concept used in WOFOST and other models
- 807 • Validation data is poor: 1) flux tower data (latent heat flux and point-
808 based rainfall, for conversion of latent heat flux to daily AET, see p. 54
809 in [Senay 2008](#)), 2) EO data for validation have not been fully exploited,
810 and 3) reported production-area-yield data are not available historically
811 with consistent coverage and quality